

# Coherent $\pi^0$ photoproduction from ${}^4\text{He}$ <sup>1</sup>

F. Rambo<sup>a,2</sup>, P. Achenbach<sup>b</sup>, J. Ahrens<sup>b</sup>, H.-J. Arends<sup>b</sup>,  
 R. Beck<sup>b</sup>, S. J. Hall<sup>c</sup>, V. Hejny<sup>d</sup>, P. Jennewein<sup>b</sup>,  
 S.S. Kamalov<sup>e,3</sup>, M. Kotulla<sup>d</sup>, B. Krusche<sup>d</sup>, V. Kuhr<sup>a</sup>,  
 R. Leukel<sup>b</sup>, V. Metag<sup>d</sup>, R. Novotny<sup>d</sup>, V. Olmos de León<sup>b</sup>,  
 A. Schmidt<sup>b</sup>, M. Schumacher<sup>a,4</sup>, U. Siodlaczek<sup>f</sup>, F. Smend<sup>a</sup>,  
 H. Ströher<sup>b,5</sup>, J. Weiss<sup>d</sup>, F. Wissmann<sup>a</sup>, M. Wolf<sup>d</sup>

<sup>a</sup>*II. Physikalisches Institut, Universität Göttingen, Bunsenstrasse 7-9, D-37073 Göttingen, Germany*

<sup>b</sup>*Institut für Kernphysik, Universität Mainz, D-55099 Mainz, Germany*

<sup>c</sup>*Department of Physics and Astronomy, University of Glasgow, Glasgow G128QQ, UK*

<sup>d</sup>*II. Physikalisches Institut, Universität Giessen, D-35392 Giessen, Germany*

<sup>e</sup>*Institut für Kernphysik, Universität Mainz, D-55099 Mainz, Germany and Department of Physics, National Taiwan University, Taipei 10617, Taiwan*

<sup>f</sup>*Physikalisches Institut, Universität Tübingen, D-72076 Tübingen, Germany*

---

## Abstract

Differential cross sections and beam asymmetries for coherent  $\pi^0$  photoproduction from  ${}^4\text{He}$  in the  $\Delta$  energy-range have been measured with high statistical and systematic precisions using both decay photons for identifying the process. The experiment was performed at the MAInz MIcrotron using the TAPS photon spectrometer and the Glasgow/Mainz tagged photon facility. The differential cross sections are in excellent agreement with predictions based on the DWIA if an appropriate parametrization of the  $\Delta$ -nuclear interaction is applied. The beam asymmetries are interpreted in terms of degrees of linear polarization of collimated coherent bremsstrahlung. The expected increase of the degree of linear polarization with decreasing collimation angle is confirmed. Agreement with calculations is obtained on a few-percent level of precision in the maxima of the coherent peaks.

PACS classification: 25.20.Lj; 24.70+s; 29.27.Hj

*Key words:* Nuclear Reactions  ${}^4\text{He}(\gamma, \pi^0){}^4\text{He}$ ,  $E_\gamma = 200 - 400$  MeV, tagged coherent bremsstrahlung beam. Measured total and differential cross sections. New theoretical calculations taking into account in-medium modification of the  $\Delta$  resonance parameters lead to excellent agreement with the experimental data.

---

## 1 Introduction

Coherent photoproduction of  $\pi^\circ$  mesons from nuclei is an ideal tool to study fundamental properties of pion-nucleus interactions. Another important aspect in the study of this reaction is the unique opportunity to get information about modifications of the  $\Delta(1232)$ -resonance characteristics in the nuclear medium. The nucleus  ${}^4\text{He}$  is especially suited for studies of this type because it combines the well known structure of a few-body system with the large binding energy of a complex nucleus. Furthermore, because of the high excitation energy of 20 MeV of the first excited level it is comparatively easy to separate coherent from incoherent  $\pi^\circ$  photoproduction processes. The advantage of coherent  $\pi^\circ$  photoproduction as compared to, e.g., the production of charged mesons is that the nucleus is identical in the initial and final states. This eliminates complicated nuclear rearrangement processes and makes a clear-cut theoretical interpretation possible. Furthermore, the coherent  $\pi^\circ$  photoproduction process is uniformly distributed over the whole nuclear volume. This leads to a substantial enhancement of the cross section in contrast to, e.g.,  $\pi^+$  photoproduction.

In spite of the fundamental importance of this process the available experimental data were very scarce. There were only four papers available [1–4] providing few and partly controversial differential cross sections. The reason for this rather unsatisfactory experimental situation was that the experiments were extremely difficult with the previously available photon beams and photon detectors. A major step forward came with the advent of *cw* electron accelerators [5–7] and of broad-band tagging facilities [8,9] as they are now available, e.g., at MAMI in Mainz. A further large progress came with the availability of high energy-resolution and large angular-acceptance photon detectors.

The present experiment is a continuation of our previous research on coherent  $\pi^\circ$  photoproduction on  ${}^4\text{He}$  [10] performed at MAMI (Mainz) [5–9] which were mainly carried out to measure the degree of linear polarization of coherent bremsstrahlung produced via a diamond radiator [11]. In these previous investigations [10] the 48 cm  $\varnothing \times$  64 cm Mainz NaI(Tl) detector [12] has been used as a high detection-efficiency and high energy-resolution (1.5%) spectrometer for the high-energy photon emitted in an asymmetric  $\pi^\circ$  decay. The experi-

---

<sup>1</sup> supported by Deutsche Forschungsgemeinschaft (SFB 201)

<sup>2</sup> Part of a doctoral thesis

<sup>3</sup> Permanent address: Laboratory of Theoretical Physics, JINR Dubna, Head Post Office Box 79, SU-101000 Moscow, Russia

<sup>4</sup> e-mail: Martin.Schumacher@phys.uni-goettingen.de

<sup>5</sup> Present address: Institut für Kernphysik, Forschungszentrum Jülich, D-52425 Jülich, Germany

ment [10] had been carried out for two different collimation angles (half of the angular opening) of  $\theta_{coll}=0.7$  mrad and  $\theta_{coll}=0.5$  mrad of the photon beam, corresponding to  $\theta_{coll} = 1.17 \times \theta_{BH}$  and  $\theta_{coll} = 0.83 \times \theta_{BH}$  where  $\theta_{BH} = mc^2/E$  ( $m$ ,  $E$  = electron mass and energy, respectively) is the characteristic (Bethe-Heitler) angle. In this range of collimation angles a pronounced dependence of the degree of linear polarization on the collimation angle  $\theta_{coll}$  is expected and this effect was clearly observed for the first time in that experiment [10]. In parallel to the experiment a program was started to precisely calculate the degree of linear polarization including all geometrical effects like the parameters of the electron beam and the collimation of the photon beam [13]. As a result of these investigations [10,13] an agreement between measured and calculated degrees of linear polarization on a  $\approx 3\%$  level of precision was obtained.

Differing from our previous experiment [10] where one decay photon has been used to identify a  $\pi^0$  event, our present experiment carried out with the TAPS setup [14–16] at MAMI makes use of both decay photons and a much larger angular acceptance. Therefore, this latter method permits to measure the degree of linear polarization of collimated photons with higher systematic and statistical precisions than it was possible before [10,13]. Furthermore, it was possible to evaluate differential cross sections for coherent  $\pi^0$  photoproduction in wide energy and angular ranges.

After completion of the present paper a similar experiment performed by Bellini et al. [17] came to our attention. It used the LEGS tagged polarized photon beam and covers a similar, but smaller range of photon energies with a smaller number of pion production angles. Using one large  $48\text{cm} \varnothing \times 48\text{cm}$  NaI(Tl) detector for the high-energy photon and an array of smaller NaI(Tl) detectors for the low-energy photon of the asymmetric  $\pi^0$  decay it was possible to single out the coherent  $\vec{\gamma} + {}^4\text{He} \rightarrow \pi^0 + {}^4\text{He}$  production channel. The present and the previous data [17] are in a general reasonable agreement with each other except for some deviations especially at the highest energies accessible in [17], as will be shown later.

## 2 Experiment

The experiments have been carried out using the BaF<sub>2</sub> multi-detector array TAPS [14–16] at the tagged-photon facility of the A2-collaboration [8,9] installed at the microtron MAMI in Mainz [5–7]. Using a diamond crystal as radiator and positioning a collimator at a distance of 2500 mm downstream from the radiator the tagged-photon facility provides linearly polarized photons with degrees of linear polarization up to 50 – 60% [10]. The accelerator was operated at its nominal maximum energy of 855 MeV. The intensity of the photon flux is limited by the tagging technique which does not allow electron

rates in a tagger channel ( $\Delta E \approx 2 \text{ MeV}$ ) larger than  $10^6 \text{ s}^{-1}$ . Since the electron rates are strongly increasing with decreasing energies of the bremsstrahlung photons the useful photon flux can be increased by switching off unused tagger channels at low photon energies. In the present experiment the orientation of the diamond crystal was chosen such that the position of the discontinuity at the high-energy side of the coherent-bremsstrahlung spectrum produced by the most prominent reciprocal lattice vector  $[02\bar{2}]$  was located close to 360 MeV. This means that significant linear polarization appeared within the energy range between 200 MeV and 360 MeV. Therefore, the tagging channels corresponding to photon energies below 200 MeV were switched off for the purpose mentioned above.

The setup of the experiment is shown in Fig. 1. TAPS consists of 384  $\text{BaF}_2$  modules having 25 cm length and hexagonal cross section (inner diameter 5.9 cm), mounted in six blocks of 64 [19,20]. Each module is equipped with its individual veto detector in front to identify incoming charged particles. The blocks were arranged in a horizontal plane in a distance of 57 cm from the target center. Their central axes were located in the scattering plane at polar angles of  $-149^\circ$ ,  $-99^\circ$ ,  $-49^\circ$ ,  $50^\circ$ ,  $100^\circ$  and  $151^\circ$ , respectively. Additional 120  $\text{BaF}_2$  modules were mounted in the forward direction symmetrically around the photon beam to build a hexagonal forward wall (FW) which covered a range of polar angles from  $2^\circ$  to  $19^\circ$ . The FW modules are of the phoswich type with a plastic detector mounted directly onto the crystal. The light output from both parts is viewed by the same photomultiplier tube. This gives an excellent identification of charged particles in addition to that via the pulse-shape discrimination provided by  $\text{BaF}_2$ .

The liquid helium target had a diameter of 3 cm and a length of 10 cm, corresponding to about  $1.86 \times 10^{23}$  nuclei/cm<sup>2</sup>. The target cell was made of Kapton and was mounted in a large ( $\text{Ø} 90 \text{ cm}$ ), evacuated scattering chamber of carbon fiber to minimize scattering, conversion and energy loss between target and detector. For automatic refilling, the Kapton cell was connected to a 5 liter  $^4\text{He}$  Dewar vessel contained in a liq.  $\text{N}_2$  shield above the scattering chamber. Several layers of superisolation foil were used to protect the target from thermal radiation. With these precautions an uninterrupted measurement was possible for 9 h.

Three different collimators having diameters of 3 mm, 4 mm and 6 mm were used to study the effect of collimation on the degree of linear polarization. In order to obtain approximately the same statistical precision in the three measurements, the total beam time of 125 h on the target was subdivided into three periods of 57, 43 and 25 h, respectively.

### 3 Data analysis and results

The two-photon decay was used to identify neutral pions. In the evaluation of data, events were selected which contained at least two coincident photons, being unambiguously identified using pulse-shape analysis, information from the charged-particle veto detectors, and time-of-flight analysis.

As a first step to identify  $\pi^\circ$  mesons from coincident (within a time window of 0.7 ns) photon pairs in two different TAPS blocks, spectra of invariant masses  $m_{\gamma\gamma}$  were constructed where the invariant mass is given by

$$m_{\gamma\gamma} = \sqrt{2E_1E_2(1 - \cos \Phi)}, \quad (1)$$

with  $E_1$  and  $E_2$  being the photon energies and  $\Phi$  the angle between the two photons. Since most of the two-photon events are due to  $\pi^\circ$  or  $\eta$  decays, the spectrum of invariant masses contains two pronounced peaks in addition to a small combinatoric background from events with more than two photons in the time window. These peaks are slightly asymmetric because of the asymmetric response function of the BaF<sub>2</sub> detectors [21]. To take care of this, also the window of accepted events around the invariant mass of 135 MeV had to be chosen asymmetric, i. e. from 90 to 160 MeV.

Because of the high angular resolution of TAPS the opening angle  $\Phi$  between two decay photons has been used to separate coherent from incoherent  $\pi^\circ$  photoproduction processes. For this purpose use was made of the relation

$$\Phi_{min} = 2 \arccos \left( \frac{\sqrt{(E_{\pi^\circ}^{lab})^2 - m_{\pi^\circ}^2}}{E_{\pi^\circ}^{lab}} \right) \quad (2)$$

between the minimum opening angle  $\Phi_{min}$  which corresponds to the symmetric two-photon decay and the  $\pi^\circ$  energy  $E_{\pi^\circ}^{lab}$  in the laboratory. Since all incoherent processes lead to a breakup of the helium nucleus, the respective  $\pi^\circ$  mesons have at least 20 MeV less energy than the coherently produced ones for a given and, in the following discussion, fixed primary photon energy. Correspondingly, the opening angles  $\Phi$  from incoherent processes are shifted to distinctly higher values (typically by 3 times the angular resolution). This shift defines, via Eq. (2), a range of opening angles  $\Phi$  which only contains coherently produced  $\pi^\circ$  mesons.

For the verification of the effectiveness of the procedure of separating coherent from incoherent events described above, use has been made of an analysis of the “missing energy” of the event which makes an explicit use of the energy

information provided by the tagger. Assuming coherent  $\pi^\circ$  photoproduction the  $cm$  energy of the  $\pi^\circ$  meson can be calculated via

$$E_{\pi^\circ}^*(E_\gamma) = \frac{s + m_{\pi^\circ}^2 - m_{He}^2}{2\sqrt{s}} \quad (3)$$

from the energy  $E_\gamma$  of the primary photon, where  $\sqrt{s} = \sqrt{2E_\gamma m_{He} + m_{He}^2}$  is the total energy in the  $cm$  system and  $m_{He}$  the mass of the He nucleus. On the other hand the same energy can be obtained via Lorentz transformation from the measured energies  $E_1$  and  $E_2$  and emission angles  $\Theta_1$  and  $\Theta_2$  of the decay photons in the laboratory system via

$$E_{\pi^\circ}^*(\gamma_1, \gamma_2) = \gamma(E_1 + E_2 - \beta(E_1 \cos \Theta_1 + E_2 \cos \Theta_2)), \quad (4)$$

with  $\beta = E_\gamma/(E_\gamma + m_{He})$  and  $\gamma = \sqrt{1 - \beta^2}$ . The difference of the two energies

$$\Delta E_{\pi^\circ} = E_{\pi^\circ}^*(\gamma_1, \gamma_2) - E_{\pi^\circ}^*(E_\gamma) \quad (5)$$

is the ‘‘missing energy’’ which should be zero in case of coherent  $\pi^\circ$  photoproduction for an infinitely high precision of the experimental quantities. The verification of the effectiveness of the procedure of separating coherent from incoherent processes is illustrated in Fig. 2, where numbers of events are shown as a function of the missing energy  $\Delta E_{\pi^\circ}$  for the four primary photon energies of  $E_\gamma = 224, 294, 320$  and  $366$  MeV. The upper curves contain the numbers of events without cuts in the spectra of opening angles  $\Phi$  as described in the preceding paragraph. These curves contain a peak structure around zero missing energy which is mainly due to coherent  $\pi^\circ$  photoproduction and a tail at the negative-energy side which is due to incoherent  $\pi^\circ$  photoproduction. The two lower curves are (i) experimental numbers of events after the cuts in the spectra of opening angles  $\Phi$  are made, and (ii) completely analogously simulated [22] numbers of events where the simulation is carried out under the premise of coherent  $\pi^\circ$  photoproduction. These two lower curves are adjusted to each other to give the same area. This, apparently, leads to a very good overall agreement of the two distributions, thus proving that indeed the respective experimental data are due to coherent  $\pi^\circ$  photoproduction only. A further quantity which is obtained from the simulation [22] is the detection efficiency of the detector which relates numbers of events to differential cross sections. Using this detection efficiency the experimental differential cross sections shown in Figs. 3 and 4 and in Table 1 are obtained. The errors given are statistical errors only. Table 2 shows the total cross sections. The total systematic error of the cross section is estimated to be 7%. It stems from the following contributions:

(i) The detection efficiency of the TAPS apparatus: 3%,

- (ii) the analysis cuts in the pulse-shape and time-of-flight spectra: 5 %,
- (iii) the tagging efficiency for coherent bremsstrahlung which is more strongly influenced by beam instabilities than the one for incoherent bremsstrahlung: 3%,
- (iv) dead-time corrections of the photon flux: 1.5 % , and
- (v) target thickness: 2%.

As is illustrated by the reduction of the numbers of experimental events shown in the peaks around zero missing energy of Fig. 2, the cuts on the opening angle  $\Phi$  have the unavoidable side effect of decreasing the acceptance of the TAPS detector. In the angular ranges between the TAPS blocks the acceptance almost drops to zero. This leads to gaps in the experimental differential cross sections close to the maxima of the angular distributions, as can be seen in part of the experimental data shown in Figs. 3 and 4. Fortunately, the differential cross sections are smooth functions of polar angle so that the gaps may be safely bridged by interpolation.

The data analysis described so far averages over the two directions (vertical and horizontal) of linear polarization so that differential cross sections for unpolarized photons are obtained. In a further step of analysis use has been made of the linear polarization provided by coherent bremsstrahlung and of the properties of coherent  $\pi^0$  photoproduction on  $^4\text{He}$  as a polarimeter for measuring the degree of linear polarization on an absolute scale. These latter properties are provided by the fact that both the nucleus and the  $\pi^0$  meson have no spins, so that  $\pi^0$  mesons are emitted exclusively as  $p$  waves through  $M1$  excitation of the  $\Delta$  resonance, a channel which is already strongly favored for the free nucleon. As a consequence, the degree of linear polarization of the photon beam is completely transferred to the azimuthal asymmetry of the  $\pi^0$  mesons. In this case the general expression for the differential cross section in the  $cm$  frame can be given by

$$\frac{d\sigma}{d\Omega} = |(\vec{\epsilon} \times \hat{k}) \cdot \hat{q}|^2 |F(\vec{q}, \vec{k})|^2, \quad (6)$$

where  $\vec{\epsilon}$  denotes the polarization vector,  $\hat{k}$  the direction of the photon and  $\hat{q}$  the direction of the pion. The function  $F(\vec{q}, \vec{k})$  is a polarization-independent normalization factor.

The azimuthal acceptance of TAPS is limited to angular intervals of  $\Delta\varphi^{max} = \pm 25^\circ$  width around  $\varphi = 0^\circ$  and  $\varphi = 180^\circ$ , i.e., above and below the horizontal reaction plane on both sides of the photon beam. In order to make use of the full sizes of these intervals without losing information, the azimuthal distributions  $N_V(\varphi)$  and  $N_H(\varphi)$  of coherent  $\pi^0$  events were determined separately for each tagger channel. These two quantities  $N_V(\varphi)$  and  $N_H(\varphi)$  are the numbers of events from coherent  $\pi^0$  photoproduction as functions of the

azimuthal angle  $\varphi$  of the  $\pi^0$  meson with the electric vector being preferentially vertical (vertical polarization V) and horizontal (horizontal polarization H), respectively, normalized to the same numbers of primary photons. The angular characteristic given by Eq. (6) predicts that the numbers of events  $N_V(\varphi)$  are larger than the numbers of events  $N_H(\varphi)$  with the intensity ratio being determined by the degree of linear polarization (in case of complete linear polarization  $N_H(\varphi)$  would be zero). The degree of linear polarization was evaluated via

$$P(E_\gamma) = \frac{1}{\cos 2\varphi} \frac{N_V(\varphi) - N_H(\varphi)}{N_V(\varphi) + N_H(\varphi)} \quad (7)$$

using angular bins of  $\Delta\varphi^{bin} = 3^\circ$  widths. As expected, Eq. (7) neither contains the efficiency of the detector nor the absolute value of the photon flux. This fact to a large extent removes the systematic errors discussed above in connection with the differential cross sections. The factor  $1/\cos 2\varphi$  corrects for the azimuthal distribution of the  $\pi^0$  mesons and is equal to 1 in case the  $\pi^0$  meson is emitted exactly in the horizontal plane. The final result for the degree of linear polarization in each tagger channel is obtained by averaging the results obtained from the expression on the r.h.s. of Eq. (7) over the angular bins  $\Delta\varphi^{bin}$  between  $\Delta\varphi^{max} = -25^\circ$  and  $\Delta\varphi^{max} = +25^\circ$ .

## 4 Discussion

### 4.1 Cross sections for coherent $\pi^0$ photoproduction

The differential cross sections obtained in the present experiment for photon energies between 200 MeV and 400 MeV are compared with previous experimental data [1–4,17] and with theoretical predictions [18]. Apparently, the present data are of considerable superiority to the previous ones, both with respect to self-consistency and with respect to completeness. Where available, the BNL data [17] are in a general reasonable agreement with the present ones except for some deviations especially at the highest energies accessible in [17]. The experimental data are compared with predictions [18] based on an extended version of the distorted wave impulse approximation (DWIA) [23–26]. In this approach the elementary process is described by the recently developed unitary isobar model [27]. Medium effects are considered by introducing a phenomenological  $\Delta$  self-energy. This allows to incorporate these effects in a self-consistent way with regard to both the “bare”  $\gamma N\Delta$  vertices and  $\Delta$  excitations due to pion rescattering.

Without going into details here, the following points should be discussed: In



Figs. 3 and 4 where the differential cross sections are shown, the dashed curves represent the results of the distorted wave impulse-approximation (DWIA). These predictions apparently are not in agreement with the experimental data especially for energies not too far away from the maximum of the  $\Delta$  resonance. The inclusion of  $\Delta$ -nuclear interaction effects (or  $\Delta$  self energy as introduced in [18]) in the free  $\Delta$  propagator leads to an almost perfect agreement between data and predictions showing that medium modifications of the main resonance characteristics (width and position) supposedly take care of that part of the reaction mechanism which is missing in the DWIA. To give a quantitative information about the  $\Delta$ -nuclear interaction we quote from ref. [18] the  $\Delta$  self-energy at  $E_\gamma = 290$  MeV, being  $V = 19 - i33$  MeV which corresponds to an increase of the  $\Delta$  resonance mass and width by 19 and 66 MeV, respectively. This result is in reasonable agreement with the results obtained in pion-nuclear scattering. It is interesting to note that by using the same parameters for the  $\Delta$  self energy also the data for coherent  $\pi^\circ$  photoproduction on  $^{12}\text{C}$  [28,29] can be described. This supports our conclusion about the general validity of the theoretical approach suggested in Ref. [18].

Fig. 5 shows the experimental total cross section for coherent  $\pi^\circ$  photoproduction obtained in the present experiment together with predictions [18]. As a dotted line this figure also contains the plane-wave impulse approximation (PWIA) which was omitted in Figs. 3 and 4 because of its large deviations from the experimental data. The comparison of the PWIA with the DWIA (dashed curve) shows that the distortion of the pion wave-function through a pion-nucleus optical potential takes care of the largest part of the discrepancy between experiment and prediction. The final adjustment, then, is achieved by the introduction of the medium effects in the  $\Delta$  propagator [18].

#### 4.2 Degrees of linear polarization

The beam asymmetry measurements have been used to calculate the degree of linear polarization of collimated coherent bremsstrahlung. The experimental results are shown in Fig. 6 together with predictions, the latter ones calculated on an absolute scale by the method described in detail in [13]. Above 300 MeV, i.e. close to the maximum polarization, the calculation fits the measured data precisely, whereas below 300 MeV the calculation underestimates the measured degree of linear polarization by up to 0.03 (absolute value). This effect appears to increase with decreasing collimation angle and is especially pronounced for  $\theta_{coll} = 0.6$  mrad. Here we find that the predictions systematically underestimate the data in the whole range between 200 and 300 MeV. This effect had already been observed in our previous investigation [10] but was to some extent masked by the lower statistical precision achieved in that experiment for the smallest collimation angle. An elaborate investigation car-

ried out in the present work showed that this systematic deviation cannot be explained by geometrical imperfections of the collimation system, i.e. it can neither be explained by a slightly decentral placement of the collimator nor by effects related with the beam properties.

It is desirable to clear up the physical origin of the remaining discrepancies between predictions and experimental data for the degree of linear polarization. Nevertheless, from the point of view of the application of collimated coherent bremsstrahlung as a source of linearly polarized photons the achieved precision is quite satisfactory. The argument for this is that in the region of large linear polarization, which is the most important one for practical applications, the agreement between experiment and calculation is perfect. The measurement of linear polarization may be improved by on-line monitoring of the intensity spectrum of coherent bremsstrahlung and, furthermore, by developing reliable methods to convert the intensity spectrum directly into that of linear polarization.

## 5 Summary and conclusion

Differential cross sections for coherent  $\pi^0$  photoproduction on  $^4\text{He}$  in the energy range between 200 MeV and 400 MeV were measured with very high statistical and systematic precisions. The experimental data are compared with predictions obtained on the basis of the DWIA. These predictions are in perfect agreement with the experimental data if appropriate medium modifications of the  $\Delta(1232)$ -resonance width and position are taken into account through a semiempirical procedure.

Making use of the properties of coherent  $\pi^0$  photoproduction as a polarimeter, the degree of linear polarization of coherent bremsstrahlung has been measured as a function of the collimation angle  $\theta_{coll}$  of the photons. Satisfactory results are obtained with respect to the utilization of coherent bremsstrahlung as a source of linearly polarized photons. However, there remain minor deviations of the measured polarization data from predicted ones which need to be clarified.

## References

- [1] J.W. Staples, Ph.D. thesis, University of Illinois, unpublished (1969)
- [2] J. Lefrançois, P. Lehmann, J. P. Repellin, *Nuovo Cim.* 65A (1970) 333
- [3] D.R. Tieger, E. C. Booth, J. P. Miller, B. L. Roberts, J. Comuzzi, G. W. Dodson, S. Gilad, R. P. Redwine, *Phys. Rev. Lett.* 53 (1984) 755
- [4] P.S. Anan'in, I. V. Glavanakov, M. N. Gushtan, *Yad. Fiz.* 41 (1985) 1393, translated in *Sov. J. Nuclear Phys.* 41 (1985) 883
- [5] H. Herminghaus, A. Feder, K.H. Kaiser, W. Manz, H. v.d. Schmitt, *Nucl. Instrum. Methods* 138 (1976) 1
- [6] H. Herminghaus, K.H. Kaiser, U. Ludwig, *Nucl. Instrum. Methods*, A 187 (1981) 103
- [7] H. Herminghaus, *Proc. 1990 Lin. Accel. Conf.* (Albuquerque, USA, 1990)
- [8] I. Anthony, J. D. Kellie, S. J. Hall, G. J. Miller, J. Ahrens, *Nucl. Instrum. Methods. A* 301 (1991) 230
- [9] S.J. Hall, G.J. Miller, R. Beck, P. Jennewein, *Nucl. Instrum. Methods A* 368 (1996) 698
- [10] A. Kraus, O. Selke, F. Rambo, G. Galler, M. Schumacher, F. Smend, R. Wichmann, F. Wissmann, S. Wolf, J. Ahrens, H.-J. Arends, R. Beck, J. Peise, *Phys. Rev. Lett.* 17 (1997) 3834
- [11] D. Lohmann, J. Peise, J. Ahrens, I. Anthony, H.-J. Arends, R. Beck, R. Crawford, A. Hünger, K.H. Kaiser, J.D. Kellie, Ch. Klümper, H.-P. Krahn, A. Kraus, U. Ludwig, M. Schumacher, O. Selke, M. Schmitz, M. Schneider, F. Wissmann, S. Wolf, *Nucl. Instrum. Methods A* 343 (1994) 494
- [12] F. Wissmann, J. Peise, M. Schmitz, M. Schneider, J. Ahrens, I. Anthony, R. Beck, B. Dolbilkin, S.J. Hall, F. Härter, S. Herdade, J. Herrmann, A. Hünger, P. Jennewein, J.D. Kellie, R. Kondratjev, H.-P. Krahn, K.-H. Krause, V. Kusnetzov, V. Lisin, G.J. Miller, A. Polonski, M. Schumacher, J. Sobolewski, Th. Walcher, A. Zabrodin, *Phys. Lett. B* 335 (1994) 119
- [13] F. Rambo, G. Galler, A. Kraus, M. Schumacher, F. Smend, F. Wissmann, S. Wolf, J. Ahrens, H.-J. Arends, R. Beck, H.-P. Krahn, J. Peise, *Phys. Rev. C* 58 (1998) 489
- [14] R. Novotny, R. Riess, R. Hingmann, H. Ströher, R. D. Fischer, G. Koch, W. Kühn, V. Metag, R. Mühlhans, U. Kneissl, W. Wilke, B. Haas, J. R. Vivien, R. Beck, B. Schoch, Y. Schutz, *Nucl. Instrum. Methods A* 262 (1987) 340
- [15] R. Novotny for the TAPS collaboration, *IEEE Trans. Nucl. Sci.* 38 (1991) 379
- [16] R. Novotny, W. Döring, V. Hejny, M. Kotulla, B. Krusche, V. Metag, M. Nold, H. Ströher, M. Wolf, *IEEE Trans. Nucl. Sci.* 43 (1996) 1260

- [17] V. Bellini, M. Capogni, A. Caracappa, L. Casano, A. D'Angelo, F. Ghio, B. Girolami, S. Hoblit, L. Hu, M. Khandaker, O. C. Kistner, L. Miceli, D. Moricciani, A. M. Sandorfi, C. Schaerf, M. L. Sperduto, C. E. Thorn, *Nuclear Phys. A* 646 (1999) 55
- [18] D. Drechsel, L. Tiator, S.S. Kamalov, Shin Nan Yang, *Nucl. Phys. A* (to be published)
- [19] B. Krusche, J. Ahrens, G. Anton, R. Beck, M. Fuchs, A. R. Gabler, F. Härter, S. Hall, P. Harty, S. Hlavac, D. MacGregor, C. McGeorge, V. Metag, R. Owens, J. Peise, M. Röbig-Landau, A. Schubert, R. S. Simon, H. Ströher, V. Tries, *Phys. Rev. Lett.* 74 (1995) 3736
- [20] V. Hejny, P. Achenbach, J. Ahrens, R. Beck, S. Hall, M. Kotulla, B. Krusche, V. Kuhr, R. Leukel, V. Metag, R. Novotny, V. Olmos de León, R.O. Owens, F. Rambo, A. Schmidt, M. Schumacher, U. Siodlaczek, H. Ströher, F. Wissmann, J. Weiß, M. Wolf, *Eur. Phys. Journ.* (to be published)
- [21] A.R. Gabler, W. Döring, M. Fuchs, B. Krusche, V. Metag, R. Novotny, M. Röbig-Landau, H. Ströher, V. Tries, C. Molenaar, H. Löhner, J. H. G. van Pol, A. Raschke, M. Šumbera, L. B. Venema, H. W. Wilschut, R. Averbek, W. Niebur, A. Schubert, R. S. Simon, R. Beck, J. Peise, G. J. Miller, R. O. Owens, G. Anton, *Nucl. Instrum. Methods A*346 (1994) 168
- [22] R. Brun et al., *GEANT 3*, Version 3.21, CERN Program Library (1994)
- [23] A.A Chumbalov, S. S. Kamalov, *Phys. Lett. B*196 (1987) 23.
- [24] M. Gmitro, S. S. Kamalov, R. Mach, *Phys. Rev. C* 36(1987) 1105.
- [25] S.S. Kamalov, T. D. Kaipov, *Phys. Lett. B* 162 (1985) 260.
- [26] S.S. Kamalov, L. Tiator, C. Bennhold, *Phys. Rev. C* 55 (1997) 98.
- [27] D. Drechsel, O. Hanstein, S. S. Kamalov, L. Tiator, *Nucl. Phys. A* 645 (1999) 145
- [28] H.J. Arends, N. Floss, A. Hegerath, B. Mecking, G. Nöldeke, R. Stenz, *Z. Phys. A*311 (1983) 367.
- [29] M. Schmitz, Ph.D. thesis, University of Mainz, unpublished (1996).

Table 1

Unpolarized differential cross sections (in the  $cm$  system) for coherent  $\pi^0$  photoproduction on  ${}^4\text{He}$  in units of  $\mu\text{b}/\text{sr}$ . First column:  $\vartheta_{cm}$  production angle in degrees. Following columns: cross sections with  $1\sigma$  statistical errors for the intervals of photon laboratory energy (in MeV) given on top of each column.

$\vartheta_{cm}$	201-210	211-222	223-234	235-246	247-258	259-270
7	0.1 (0.1)	0.3 (0.1)	0.4 (0.1)	0.4 (0.2)	1.8 (0.3)	1.3 (0.3)
12	2.1 (0.1)	2.9 (0.1)	3.6 (0.2)	5.4 (0.3)	6.2 (0.3)	7.5 (0.3)
17	4.2 (0.2)	5.5 (0.2)	6.9 (0.2)	9.2 (0.3)	11.2 (0.3)	13.2 (0.3)
22	6.9 (0.2)	8.3 (0.2)	10.6 (0.2)	14.3 (0.3)	16.8 (0.3)	20.3 (0.3)
27	9.2 (0.3)	11.5 (0.3)	14.0 (0.3)	18.6 (0.4)	22.4 (0.4)	26.6 (0.4)
32	11.4 (0.3)	13.3 (0.3)	15.8 (0.4)	22.5 (0.4)	28.7 (0.4)	33.2 (0.4)
37	12.7 (0.4)	15.9 (0.4)	18.9 (0.4)	26.4 (0.5)	33.2 (0.5)	39.7 (0.6)
42	15.0 (0.4)	17.7 (0.4)	23.6 (0.5)	29.9 (0.6)	37.6 (0.7)	43.2 (0.7)
47	15.9 (0.4)	–	–	–	–	–
62	–	–	31.5 (0.7)	41.4 (0.8)	48.0 (0.8)	54.4 (0.8)
67	–	24.7 (0.7)	34.8 (0.6)	40.7 (0.5)	46.2 (0.5)	49.2 (0.5)
72	19.5 (0.6)	25.7 (0.6)	32.5 (0.5)	39.0 (0.5)	42.7 (0.4)	45.3 (0.4)
77	20.4 (0.5)	24.4 (0.4)	30.2 (0.4)	36.5 (0.4)	39.5 (0.4)	41.0 (0.4)
82	19.2 (0.4)	23.8 (0.4)	27.5 (0.4)	32.7 (0.4)	35.2 (0.4)	35.8 (0.3)
87	17.6 (0.3)	20.1 (0.3)	24.9 (0.3)	29.1 (0.4)	30.8 (0.4)	30.3 (0.3)
92	17.0 (0.3)	19.1 (0.3)	22.0 (0.3)	26.0 (0.4)	27.4 (0.4)	26.6 (0.4)
97	14.9 (0.3)	16.7 (0.3)	19.3 (0.3)	21.9 (0.4)	22.5 (0.4)	21.7 (0.5)
102	13.3 (0.2)	14.1 (0.2)	15.6 (0.3)	17.1 (0.3)	16.4 (0.4)	15.4 (0.5)
107	11.9 (0.2)	12.7 (0.2)	13.0 (0.3)	14.3 (0.3)	12.6 (0.4)	12.0 (0.4)
112	10.3 (0.2)	11.1 (0.2)	11.8 (0.3)	11.9 (0.3)	10.2 (0.3)	8.9 (0.3)
117	8.7 (0.2)	8.8 (0.2)	9.2 (0.2)	9.6 (0.2)	8.2 (0.2)	6.3 (0.2)
122	7.0 (0.2)	7.8 (0.2)	7.4 (0.2)	7.0 (0.2)	6.6 (0.2)	4.8 (0.2)
127	6.1 (0.3)	6.0 (0.2)	6.1 (0.3)	6.4 (0.2)	5.0 (0.2)	3.6 (0.2)
132	5.1 (0.3)	5.1 (0.2)	5.5 (0.3)	4.9 (0.3)	3.7 (0.2)	2.5 (0.1)
137	3.3 (0.2)	3.9 (0.2)	3.1 (0.3)	3.2 (0.3)	2.9 (0.2)	1.9 (0.2)
142	3.1 (0.2)	3.5 (0.2)	2.8 (0.4)	0.8 (0.3)	1.0 (0.2)	0.5 (0.2)
147	2.8 (0.2)	2.3 (0.2)	1.5 (0.3)	–	–	–

Table 1  
(continued)

$\vartheta_{cm}$	271-282	283-294	295-308	309-318	319-330	331-342
7	2.2 (0.3)	3.4 (0.3)	2.9 (0.2)	4.5 (0.3)	4.2 (0.3)	2.5 (0.3)
12	8.8 (0.3)	10.3 (0.3)	10.3 (0.3)	11.9 (0.4)	11.6 (0.3)	10.9 (0.3)
17	15.5 (0.3)	16.7 (0.3)	19.0 (0.3)	20.2 (0.4)	20.5 (0.3)	20.5 (0.3)
22	23.0 (0.4)	24.7 (0.4)	27.3 (0.4)	29.2 (0.5)	29.3 (0.4)	30.7 (0.4)
27	30.0 (0.4)	32.6 (0.4)	35.6 (0.4)	38.4 (0.5)	37.9 (0.4)	37.4 (0.4)
32	36.9 (0.4)	40.3 (0.4)	42.7 (0.4)	46.3 (0.6)	44.6 (0.4)	43.8 (0.4)
37	44.1 (0.5)	45.9 (0.5)	49.3 (0.5)	50.5 (0.6)	50.0 (0.5)	47.8 (0.5)
42	47.7 (0.7)	50.6 (0.6)	53.0 (0.6)	54.4 (0.8)	51.9 (0.6)	50.0 (0.5)
47	52.2 (1.2)	52.6 (1.0)	54.2 (0.9)	53.5 (1.0)	51.7 (0.7)	48.5 (0.7)
51	51.4 (3.3)	49.2 (2.4)	55.4 (2.0)	55.8 (1.9)	49.6 (1.2)	45.9 (1.1)
58	50.0 (1.6)	51.3 (1.4)	51.2 (1.4)	52.3 (1.4)	48.8 (1.0)	40.7 (0.8)
62	52.9 (0.7)	49.7 (0.6)	50.7 (0.6)	44.9 (0.7)	41.0 (0.5)	33.4 (0.4)
67	49.3 (0.5)	46.2 (0.4)	44.2 (0.4)	39.0 (0.5)	33.9 (0.3)	28.3 (0.3)
72	44.0 (0.4)	41.0 (0.4)	37.8 (0.3)	32.9 (0.4)	27.9 (0.3)	22.0 (0.2)
77	39.4 (0.3)	34.4 (0.3)	31.0 (0.3)	25.6 (0.3)	20.8 (0.2)	16.4 (0.2)
82	33.9 (0.3)	29.3 (0.3)	24.7 (0.2)	20.6 (0.3)	15.5 (0.2)	12.1 (0.2)
87	28.2 (0.3)	23.9 (0.3)	19.0 (0.2)	15.0 (0.3)	10.9 (0.2)	8.8 (0.1)
92	24.3 (0.4)	19.0 (0.3)	14.4 (0.2)	10.8 (0.3)	7.8 (0.2)	6.0 (0.1)
97	20.1 (0.5)	17.0 (0.4)	10.8 (0.3)	8.0 (0.3)	5.2 (0.2)	4.3 (0.1)
101	12.1 (0.6)	10.8 (0.8)	7.1 (0.5)	4.9 (0.4)	3.7 (0.2)	2.1 (0.2)
107	7.5 (0.5)	4.7 (0.5)	1.6 (0.3)	3.0 (0.4)	1.9 (0.2)	1.4 (0.2)
112	6.4 (0.3)	4.3 (0.2)	2.6 (0.2)	2.1 (0.2)	1.7 (0.1)	1.6 (0.1)
117	4.1 (0.2)	2.7 (0.1)	2.0 (0.1)	1.8 (0.1)	1.5 (0.1)	1.3 (0.1)
122	3.2 (0.1)	2.0 (0.1)	1.6 (0.1)	1.3 (0.1)	1.4 (0.1)	1.3 (0.1)
127	2.2 (0.1)	1.3 (0.1)	1.3 (0.1)	1.3 (0.1)	1.2 (0.1)	1.2 (0.1)
132	1.4 (0.1)	0.9 (0.1)	1.0 (0.1)	1.1 (0.1)	1.1 (0.1)	1.0 (0.1)
137	1.0 (0.1)	0.8 (0.1)	0.9 (0.1)	1.1 (0.1)	1.1 (0.1)	0.9 (0.1)

Table 1  
(continued)

$\vartheta_{cm}$	343-355	356-366	367-378	379-390	391-401
8	2.4 (0.3)	2.0 (0.4)	–	9.9 (3.5)	–
12	9.1 (0.3)	10.7 (0.4)	5.2 (0.6)	7.4 (0.8)	8.4 (1.5)
17	19.9 (0.3)	21.4 (0.4)	18.2 (0.6)	18.0 (0.7)	17.0 (0.7)
22	28.9 (0.4)	30.9 (0.4)	27.4 (0.6)	26.7 (0.6)	24.2 (0.6)
27	36.1 (0.4)	37.7 (0.4)	34.1 (0.6)	31.2 (0.5)	29.2 (0.5)
32	40.3 (0.4)	43.3 (0.5)	37.2 (0.6)	34.3 (0.5)	32.3 (0.5)
37	45.1 (0.4)	47.0 (0.5)	40.2 (0.6)	35.7 (0.6)	33.1 (0.6)
42	45.9 (0.5)	46.5 (0.6)	38.3 (0.8)	35.7 (0.8)	31.1 (0.8)
47	43.1 (0.7)	43.8 (0.9)	35.6 (1.1)	27.0 (1.1)	28.7 (1.2)
52	37.9 (1.0)	36.8 (1.3)	27.7 (1.9)	27.4 (2.2)	20.3 (2.5)
58	36.4 (0.8)	32.4 (1.0)	20.9 (1.4)	17.1 (1.8)	15.0 (2.8)
62	29.0 (0.4)	27.1 (0.5)	19.4 (0.6)	15.5 (0.7)	12.6 (0.8)
67	23.5 (0.3)	21.9 (0.3)	16.6 (0.4)	12.0 (0.4)	10.3 (0.4)
72	18.4 (0.2)	16.7 (0.2)	12.0 (0.3)	9.9 (0.3)	7.4 (0.2)
77	13.3 (0.2)	11.8 (0.2)	8.5 (0.2)	6.7 (0.2)	5.4 (0.2)
82	9.1 (0.1)	7.9 (0.1)	5.9 (0.2)	4.7 (0.2)	3.7 (0.1)
87	6.6 (0.1)	5.9 (0.1)	4.1 (0.1)	3.0 (0.1)	2.6 (0.1)
92	4.6 (0.1)	4.0 (0.1)	2.7 (0.1)	2.2 (0.1)	1.5 (0.1)
97	3.0 (0.1)	2.8 (0.1)	1.4 (0.1)	1.0 (0.1)	0.8 (0.1)
102	2.1 (0.1)	1.9 (0.1)	0.4 (0.1)	–	–
107	0.2 (0.1)	0.8 (0.1)	0.3 (0.1)	–	–
112	1.3 (0.1)	1.0 (0.1)	0.8 (0.1)	–	–
117	1.1 (0.1)	1.2 (0.1)	0.4 (0.1)	–	–
122	1.1 (0.1)	1.0 (0.1)	0.7 (0.1)	–	–

Table 2

Unpolarized total cross section  $\sigma_{tot}$  for coherent  $\pi^0$  photoproduction on  ${}^4\text{He}$  in units of  $\mu\text{b}$  as a function of the photon laboratory energy  $E_\gamma$  in MeV. The numbers in parentheses are  $1\sigma$  statistical errors.

$E_\gamma$	$\sigma_{tot}$	$E_\gamma$	$\sigma_{tot}$
206	150.0 (0.8)	313	248.1 (0.9)
216	174.5 (0.8)	325	218.7 (0.6)
229	212.6 (0.9)	337	193.1 (0.6)
241	260.3 (1.0)	349	168.9 (0.6)
253	285.2 (1.0)	361	165.7 (0.7)
265	303.2 (1.0)	372	132.5 (0.8)
277	298.3 (0.9)	385	116.0 (0.8)
289	279.3 (0.8)	397	102.8 (0.8)
301	266.1 (0.8)		



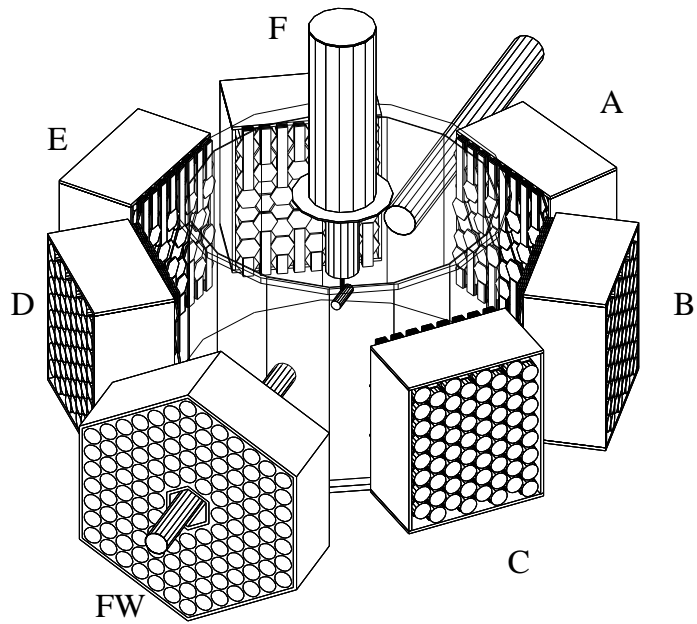


Fig. 1. The setup of the spectrometer TAPS as used for the present experiment. Six  $\text{BaF}_2$  blocks A - F and the forward wall FW are arranged around the scattering chamber which is indicated by thin lines. In the center of the scattering chamber the  $^4\text{He}$  target is shown as a horizontal cylinder. The photon beam enters the scattering chamber through the beam pipe between blocks A and F and leaves it through a hole in the forward wall FW.

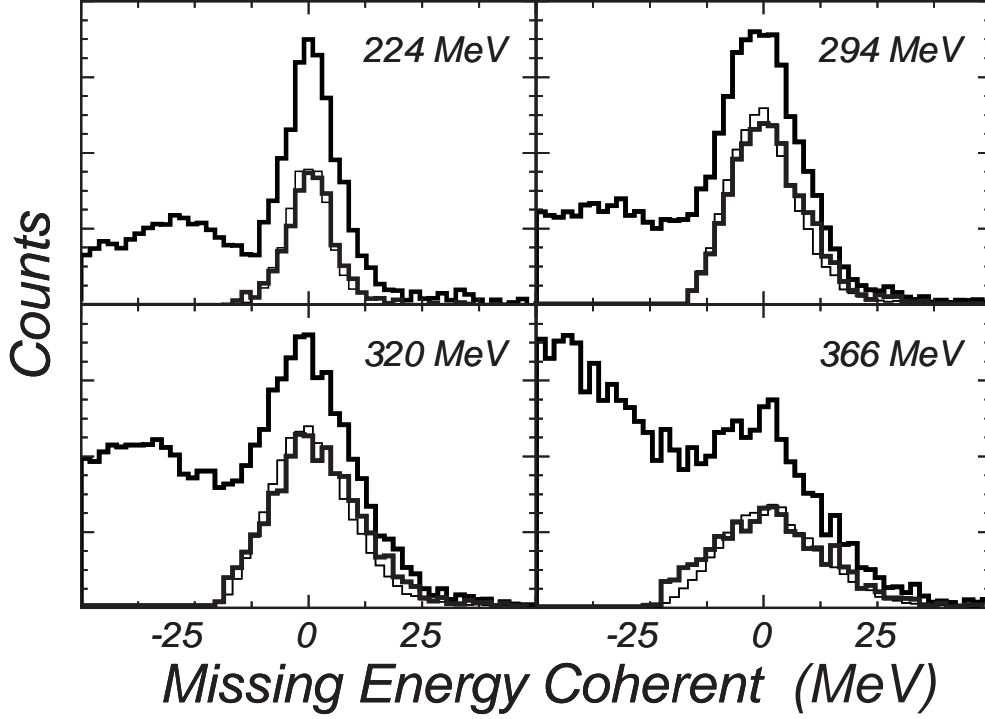


Fig. 2. Numbers of events of  $\pi^0$  photoproduction at primary photon energies of 224 MeV, 294 MeV, 320 MeV and 366 MeV versus the missing energy  $\Delta E_{\pi^0}$  calculated via Eq. (5) for the coherent kinematics. The upper distributions represented by thick solid lines contain all  $\pi^0$  events identified by the invariant mass defined in Eq. (1) of their decay photons. The lower distributions indicated by thick solid lines represent the remaining experimental events after the cut on the opening angle  $\Phi$  of the decay photons is carried out. The thin solid lower lines show the results of Monte Carlo simulations in which only coherently produced  $\pi^0$  mesons were generated.

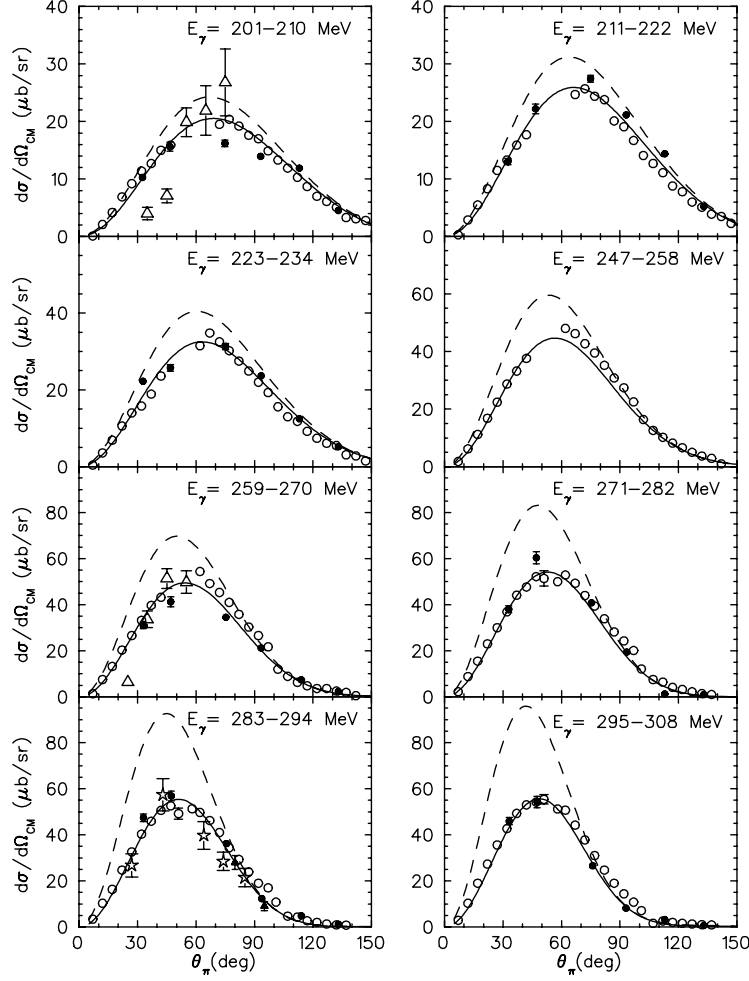


Fig. 3. Unpolarized differential cross sections for coherent  $\pi^0$  photoproduction from  ${}^4\text{He}$  for different photon energy intervals  $E_{\gamma}$  as given in the figures. Open circles: present experiment, full circles: BNL data ref. [17], open triangles: Tomsk data ref. [4], open stars: MIT data ref. [3], full triangles: ref. [2]. Dashed curves are the DWIA results of ref. [18]. The solid curves are the theoretical results obtained with the formfactor-type parameterization for the  $\Delta$  self-energy of ref. [18].

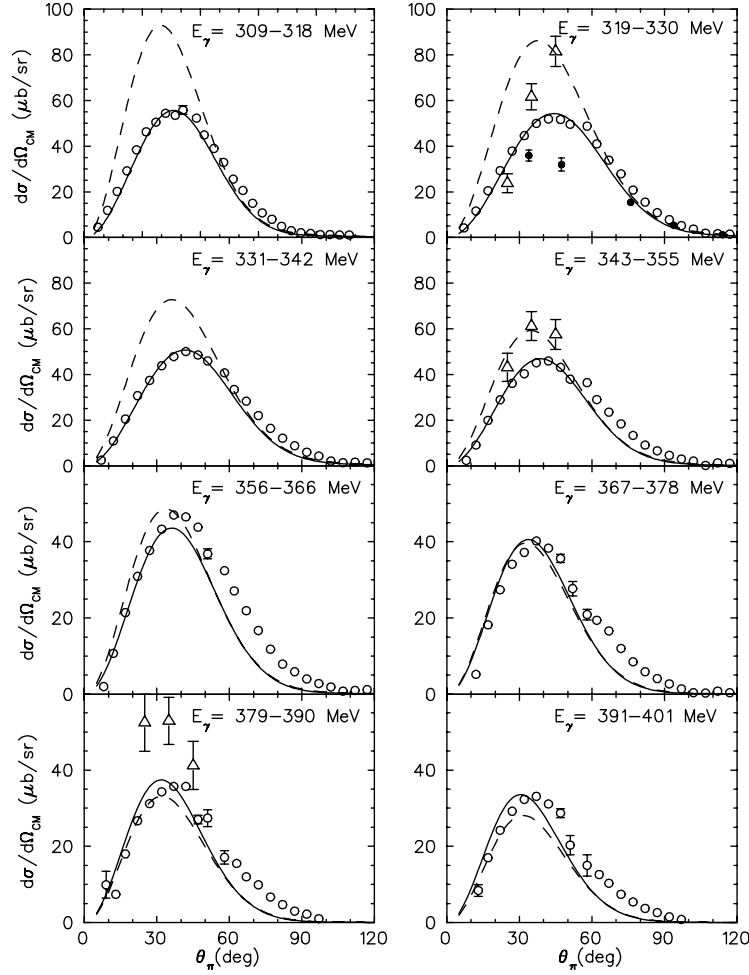


Fig. 4. Unpolarized differential cross sections for coherent  $\pi^0$  photoproduction from  ${}^4\text{He}$  for different photon energy-intervals  $E_\gamma$  as given in the figures. The notations are the same as in Figure 3.

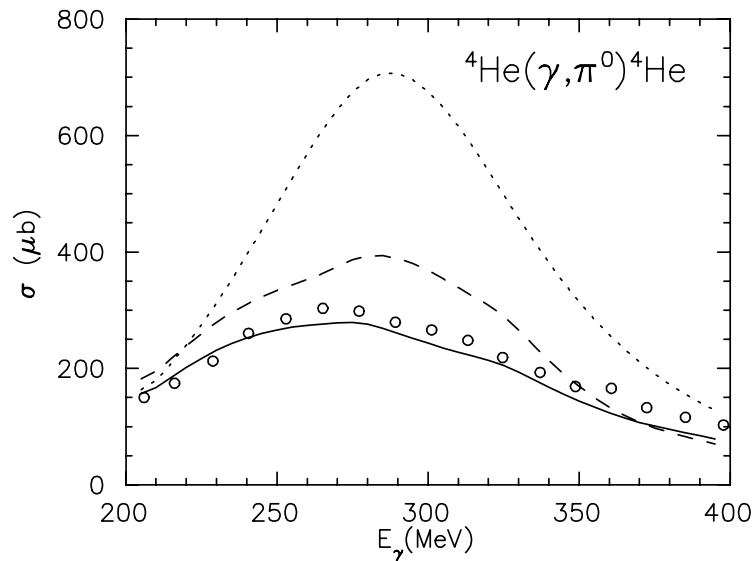


Fig. 5. Energy dependence of the total unpolarized cross section for the  ${}^4\text{He}(\gamma, \pi^0){}^4\text{He}$  reaction. The experimental data are from the present experiment. The dotted and dashed curves are the total cross sections for PWIA and DWIA, respectively, of ref. [18]. The solid curve is the result obtained with the formfactor-type parametrization for the  $\Delta$  self-energy of ref. [18]

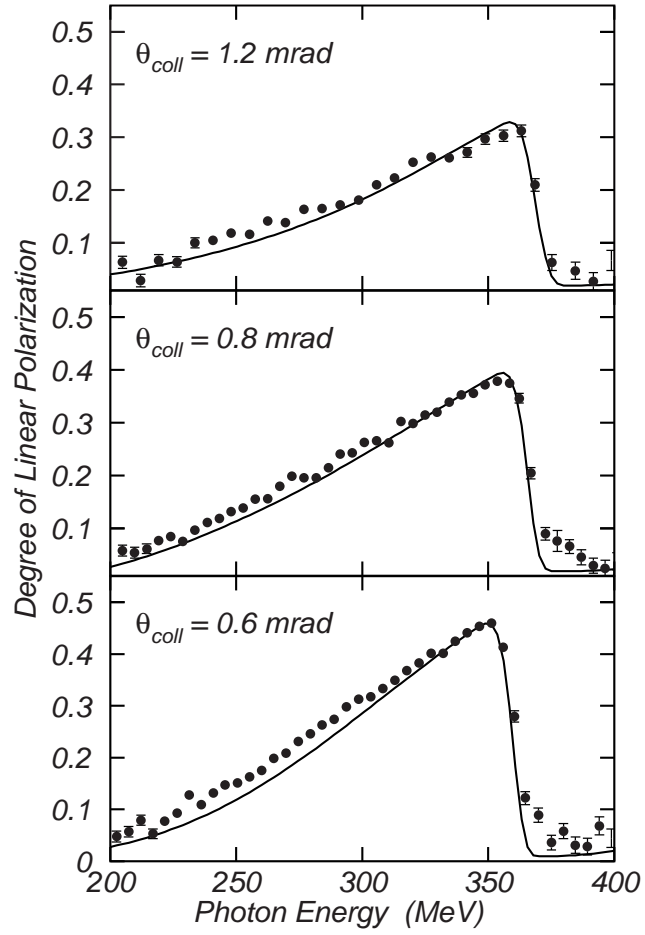


Fig. 6. The degree of linear polarization of collimated coherent bremsstrahlung using collimation angles (half of the angular opening) of  $\theta_{coll} = 1.2, 0.8$  and  $0.6$  mrad. The solid line is the result of a simulation using the method described in [13].